

## ION CHANNEL ACTIVITY IN LOBSTER SKELETAL MUSCLE MEMBRANE

MARY KATE WORDEN<sup>1\*</sup>, RAMI RAHAMIMOFF<sup>2</sup> AND EDWARD A. KRAVITZ<sup>1</sup>

<sup>1</sup>*Department of Neurobiology, Harvard Medical School, 220 Longwood Avenue, Boston, MA 02150, USA* and <sup>2</sup>*Department of Physiology, Hebrew University, Hadassah Medical School, PO Box 1172, Jerusalem, Israel 91010*

*Accepted 4 May 1993*

### Summary

Ion channel activity in the sarcolemmal membrane of muscle fibers is critical for regulating the excitability, and therefore the contractility, of muscle. To begin the characterization of the biophysical properties of the sarcolemmal membrane of lobster exoskeletal muscle fibers, recordings were made from excised patches of membrane from enzymatically induced muscle fiber blebs. Blebs formed as evaginations of the muscle sarcolemmal membrane and were sufficiently free of extracellular debris to allow the formation of gigaohm seals. Under simple experimental conditions using bi-ionic symmetrical recording solutions and maintained holding potentials, a variety of single channel types with conductances in the range 32–380 pS were detected. Two of these ion channel species are described in detail, both are cation channels selective for potassium. They can be distinguished from each other on the basis of their single-channel conductance and gating properties. The results suggest that current flows through a large number of ion channels that open spontaneously in bleb membranes in the absence of exogenous metabolites or hormones.

### Introduction

Crustacean neuromuscular preparations have been widely used for exploring the actions of hormonal substances on pre- and postsynaptic physiological processes (Dudel, 1965; Kravitz *et al.* 1980; Breen and Atwood, 1983; Atwood *et al.* 1989). These preparations offer the virtues of being easily obtained peripheral tissues, having a relatively simple excitatory and inhibitory innervation, being composed of large diameter muscle fibers and exhibiting a complex hormonal regulation of the functional effectiveness of both nerve and muscle (Fischer and Florey, 1983; Kravitz *et al.* 1985; Dixon and Atwood, 1989*a,b*; Mercier *et al.* 1990). The aim of this study was to begin the characterization of the ion channels of lobster exoskeletal muscle fiber membranes, in anticipation that part of the hormonal modulation of the effectiveness of contraction

\*Present address: Department of Molecular Physiology and Biological Physics, Box 449, Jordan Hall, University of Virginia Health Sciences Center, 1300 Jefferson Park Avenue, Charlottesville, VA 22908, USA.

Key words: ion channel, lobster, bleb, *Homarus americanus*, muscle membrane.

would be due to changes in the functional properties of individual ion channels (Bishop *et al.* 1991; Eusebi *et al.* 1988).

The richness of the hormonal regulation of lobster neuromuscular preparations makes these tissues suitable candidates for extensive studies of modulation. Four hormonal substances that cause important changes in nerve and muscle function have been found in these preparations. These are the amines serotonin and octopamine and the peptides proctolin (RYLPT) and peptide F<sub>1</sub> (TNRNFLRFamide) (Evans *et al.* 1975, 1976; Batelle and Kravitz, 1978; Schwarz *et al.* 1980, 1984; Kravitz *et al.* 1980; Kobierski *et al.* 1987; Trimmer *et al.* 1987). Studies with the amine serotonin serve to illustrate the complexity of the modulation of lobster muscle contractility. This amine is released from thoracic root neurosecretory structures directly into the general circulation, where it is carried to all peripheral tissues including muscles (Sullivan *et al.* 1977; Sullivan, 1978; Livingstone *et al.* 1981). Serotonin acts directly on muscle fibers, where it produces a contracture, enhances the strength of contractions and causes an increase in an inward calcium current (Grundfest and Reuben, 1961; Kravitz *et al.* 1980; Livingstone *et al.* 1980; Goy and Kravitz, 1989).

In this communication, we report the beginning of an investigation of the possible biophysical substrates of this type of hormonal regulation. To facilitate studies of the membrane channel properties, we adapted a procedure originally developed for vertebrate skeletal muscle (Burton *et al.* 1988), in which the enzyme collagenase is applied to muscles in an isotonic KCl solution to cause the appearance of 'blebs' along muscle fiber membranes. The bleb surfaces are free of extracellular debris, greatly increasing the probability of obtaining gigaohm seals with a patch pipette. Using the bleb technique, a detailed study of the ion channel composition of lobster muscle fiber membranes has been performed at the single channel level.

The aims of this paper are to describe the collagenase procedure used to produce membrane blebs as applied to lobster muscle membrane and to characterize several types of potassium channels observed in single-channel recordings from lobster muscle blebs.

## Materials and methods

### *Bleb formation*

The distal heads of the accessory flexor muscle of the meropodite of the first and second walking legs were dissected (attached to the exoskeleton and the central apodeme) from adult *Homarus americanus* of both sexes. Muscles were dissected in physiological lobster saline, which approximates the ionic composition of lobster hemolymph (462mmol l<sup>-1</sup> NaCl, 16mmol l<sup>-1</sup> KCl, 26mmol l<sup>-1</sup> CaCl<sub>2</sub>, 8mmol l<sup>-1</sup> MgCl<sub>2</sub>, 5mmol l<sup>-1</sup> Hepes, 11mmol l<sup>-1</sup> glucose, pH7.4; 1200mosmol l<sup>-1</sup>). The muscles were then rinsed in a saline solution to which no calcium had been added (462mmol l<sup>-1</sup> NaCl, 16mmol l<sup>-1</sup> KCl, 34mmol l<sup>-1</sup> MgCl<sub>2</sub>, 5mmol l<sup>-1</sup> Hepes, 11mmol l<sup>-1</sup> glucose, pH7.4, 1200mosmol l<sup>-1</sup>) and transferred to an enzyme solution containing 100units ml<sup>-1</sup> collagenase (Type 1A; Sigma) in 462mmol l<sup>-1</sup> KCl buffered with 5mmol l<sup>-1</sup> Hepes (pH7.8; 1100mosmol l<sup>-1</sup>). Treatment with the enzyme solution induced muscle contraction followed by relaxation. Within 1min of relaxation, the muscle was pinned out

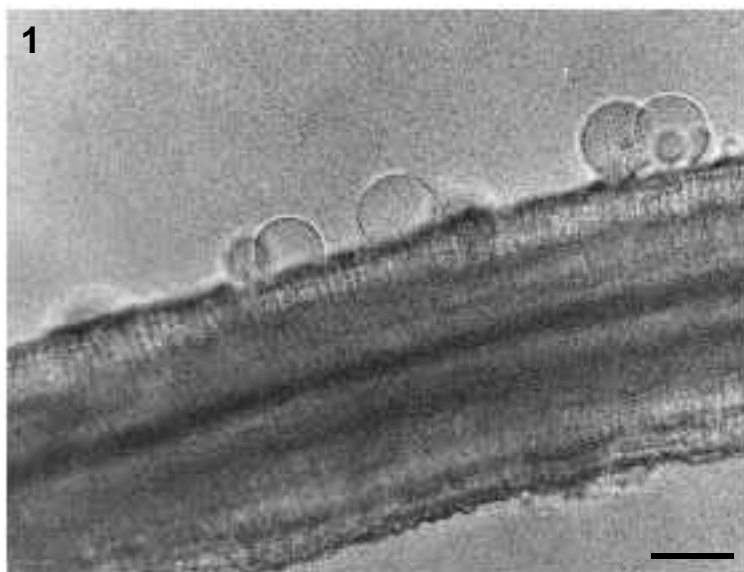


Fig. 1. Bleb formation on the surface of lobster skeletal muscle. The accessory flexor muscle of the meropodite was treated for 15min with collagenase in a solution containing an elevated level of potassium (see Materials and methods). Scale bar, 75  $\mu\text{m}$ .

in a Sylgard-coated Petri dish. Incubation in the enzyme solution continued for 20min at room temperature. The surface of individual muscle fibers began to form clear spherical blebs at this time. Finally, the enzyme solution was rinsed from the preparation and replaced with a simplified enzyme-free solution ( $462\text{mmol l}^{-1}$  KCl,  $5\text{mmol l}^{-1}$  Hepes, pH7.8).

#### *Single-channel recordings*

Patch pipettes of borosilicate glass were pulled in two stages using a Sachs-Flaming puller. Pipettes were coated with Sylgard and fire-polished, with typical pipette resistances ranging from 5 to  $10\text{M}\Omega$ . Positive pressure was applied as the pipette approached the surface of the blebs. Gigaohm seals between the patch pipette and the surface of the blebs formed readily when the positive pressure was released or when slight negative pressure was applied to the interior of the pipette. Seal formation was optimal during the first 2h following bleb formation, when blebs were transparent and the surface was free of debris. Following seal formation, the membrane patches were excised from the surface of the blebs in an inside-out configuration. Recordings of single-channel activity were made as described by Hamill *et al.* (1981) with a pipette solution containing  $462\text{mmol l}^{-1}$  KCl,  $5\text{mmol l}^{-1}$  Hepes, pH7.8. In some experiments patch pipettes were filled with lobster saline. In all experiments the seal resistance was greater than  $4\text{G}\Omega$ . Channel activity was observed in nearly all patches when a depolarizing or hyperpolarizing potential was applied to the membrane patch. Solutions were applied to the intracellular face of the patch using a horizontal array of microcapillary tubes as described by Friel and Bean (1988). The excised patch was held in the mouth of a

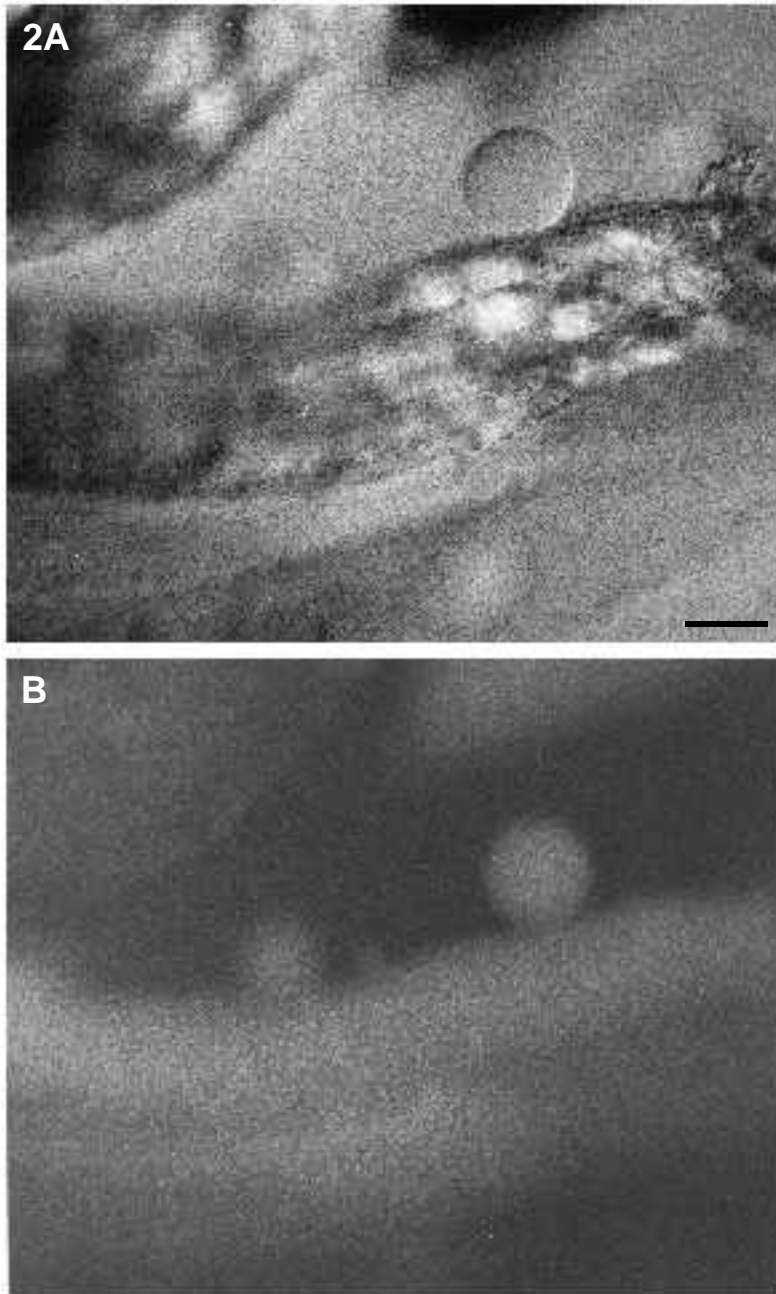


Fig. 2. (A) Muscle and blebs in phase contrast. (B) The same field visualized with fluorescence optics. The muscle was injected with Lucifer Yellow immediately prior to application of the collagenase solution. The fluorescent dye fills the interior of the blebs as well as the muscle fiber. Scale bar in A, 50  $\mu\text{m}$ .

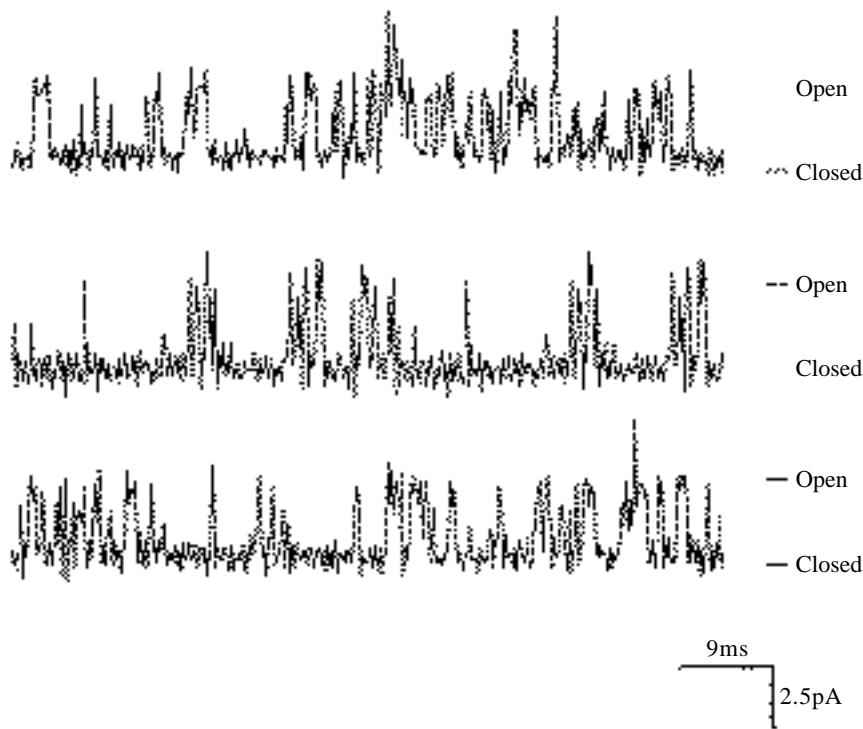


Fig. 3. Channel activity in an excised patch of membrane from lobster skeletal muscle blebs. Pipette solution: lobster saline (see Materials and methods). Bath solution:  $462\text{mmol l}^{-1}$  KCl,  $5\text{mmol l}^{-1}$  HEPES, pH7.8. Pipette potential is 0mV. Channel openings are shown as upward deflections of the current trace. Single-channel currents of several amplitudes are present in the recording.

microcapillary tube, so that a stream of solution flowed constantly over the intracellular face of the patch. Changes of solution were effected by moving the patch to the mouth of a different tube. Alterations in single-channel activity occurred within a second with each change of solution, suggesting that the excised patches were open membranes and not vesicles.

Currents were recorded using a List EPC-7 amplifier, stored on tape (Hewlett-Packard, model 3964A) and subsequently digitized at a sampling rate of 42kHz using an NEC computer. Data were filtered at 3kHz and analyzed using pClamp software (Axon Instruments, versions 4.0-5.5) to detect and analyze single channel openings.

## Results

### *Muscle fiber blebs*

Treatment of lobster skeletal muscle with an enzyme solution containing collagenase results in the appearance of membrane blebs on the extracellular surface of muscle fibers (Fig. 1). After 10–15min of incubation the blebs range in size from 5 to 100  $\mu\text{m}$ . Larger blebs predominate with longer (20–25min) incubations in collagenase solution. Two

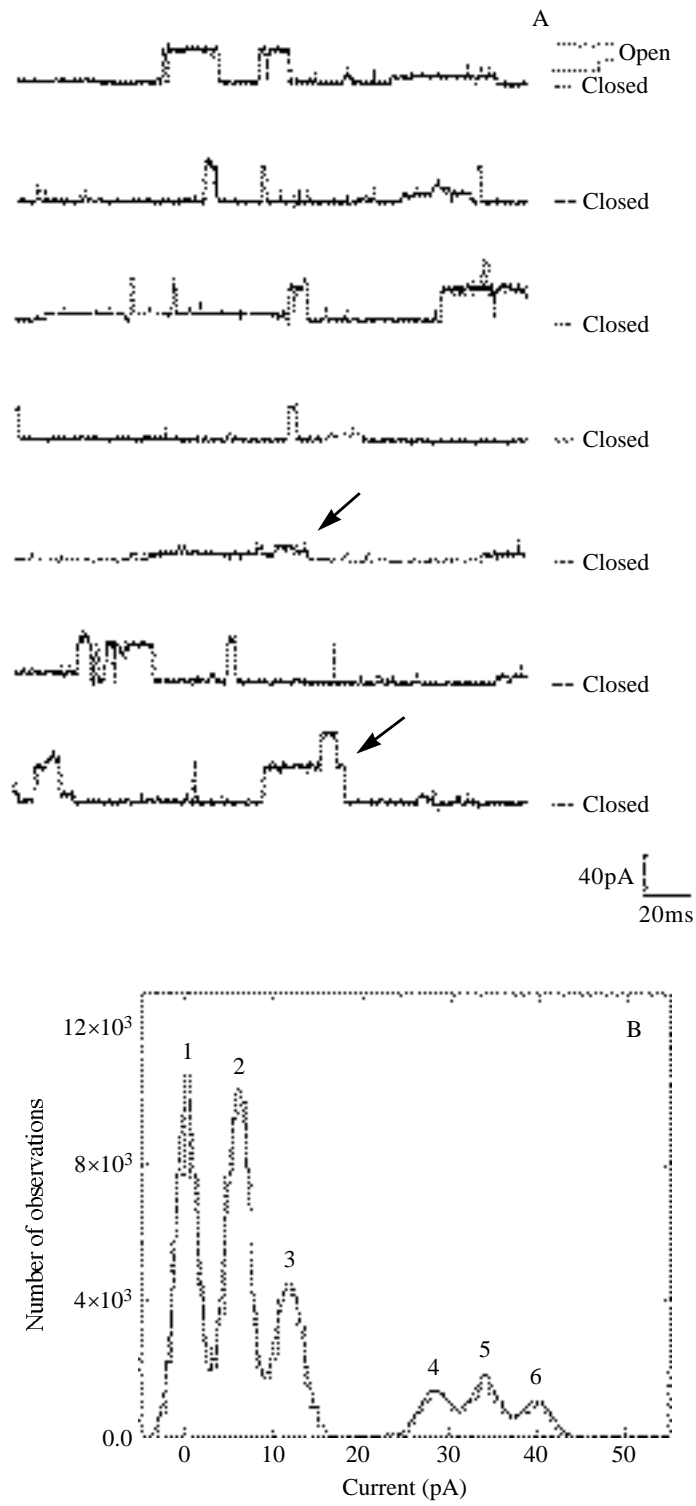


Fig. 4

lines of evidence indicate that the blebs arise from evagination of the muscle membrane as sarcolemmal contacts to internal structural elements are enzymatically disrupted. First, pressure applied *via* the patch pipette easily explodes (with positive pressure) or implodes (with negative pressure) the blebs. The fragile nature of the blebs suggests that the functional integrity of the internal cytoskeleton has been disrupted. Second, injection of the dye Lucifer Yellow into a muscle fiber prior to treatment with the collagenase solution results in diffusion of dye from the cytoplasm into the interior of the blebs (Fig. 2). The latter observation suggests that the blebs contain cytoplasmic components and that the interiors of the blebs are continuous with the muscle cytoplasm during the period of bleb formation. In addition, dye does not leak from the bleb over a 1h period, suggesting that the blebs are not generally leaky to the extracellular environment.

#### *Ion channel activity in blebs*

Several types of unitary ionic currents were detected in voltage-clamp recordings from excised inside-out patches of muscle blebs. A typical recording is shown in Fig. 3, in which the pipette was filled with lobster saline solution (to mimic the normal extracellular environment) and the intracellular face of the excised patch was bathed with a high-potassium solution (to mimic the intracellular environment). At a holding potential ( $V_{\text{pipette}}$ ) of 0mV, several channels are active in the excised patch (Fig. 3). The polarity of observed channel openings (upward) suggests that these openings result either from the net flow of cations from the bath into the pipette or from the net flow of anions from the pipette into the bath. Since the driving force for chloride ions is close to zero at this membrane potential, it is likely that these current events arise from the movement of cations.

The recordings were repeated under simplified ionic conditions where the pipette and bath solutions were identical (462mmol l<sup>-1</sup> KCl, 5mmol l<sup>-1</sup> Hepes, pH7.8). In a typical recording of this type, no channel activity is detected in the excised patch at a holding potential of 0mV as no ionic concentration gradients exist. Channel opening events appear when a potential difference is applied across the patch membrane. Fig. 4 illustrates such an experiment with  $-V_{\text{pipette}}$  equal to +60mV. Typically, several size

---

Fig. 4. (A) Channel activity in a bleb membrane patch. Pipette and bath solutions are identical: 462mmol l<sup>-1</sup> KCl, 5mmol l<sup>-1</sup> Hepes, pH7.8. Holding potential ( $-V_{\text{pipette}}$ ) is +60mV. Both large and small single-channel currents are observed, with occasional multiple openings of both channel types (arrows). (B) Amplitude histogram constructed from the raw data digitized from the experiment shown in Fig. 4A. Curve-fitting of each peak was accomplished by a non-linear least-squares fit to each Gaussian distribution. Peak 1 (centered at 0pA) corresponds to the current recorded from the patch when all the channels were apparently closed (baseline current). Peak 2 corresponds to the current flowing through a single channel (6.32±1.46pA) (mean ± s.d.). Peak 3 is current flowing through two small channels opening simultaneously (12.48±1.65pA). Peak 4 is current flowing through one large channel (30.12±2.04pA). Peak 5 is current flowing through one large and one small channel open simultaneously (total current 36.15±1.71pA). Peak 6 is current flowing through one large and two small channels (total current 42.43±2.15pA). The area under each peak was calculated as a percentage of the total area fitted by the Gaussian curves. Peak 1, 31%; peak 2, 33%; peak 3, 17%; peak 4, 7%; peak 5, 7%; peak 6, 5%.

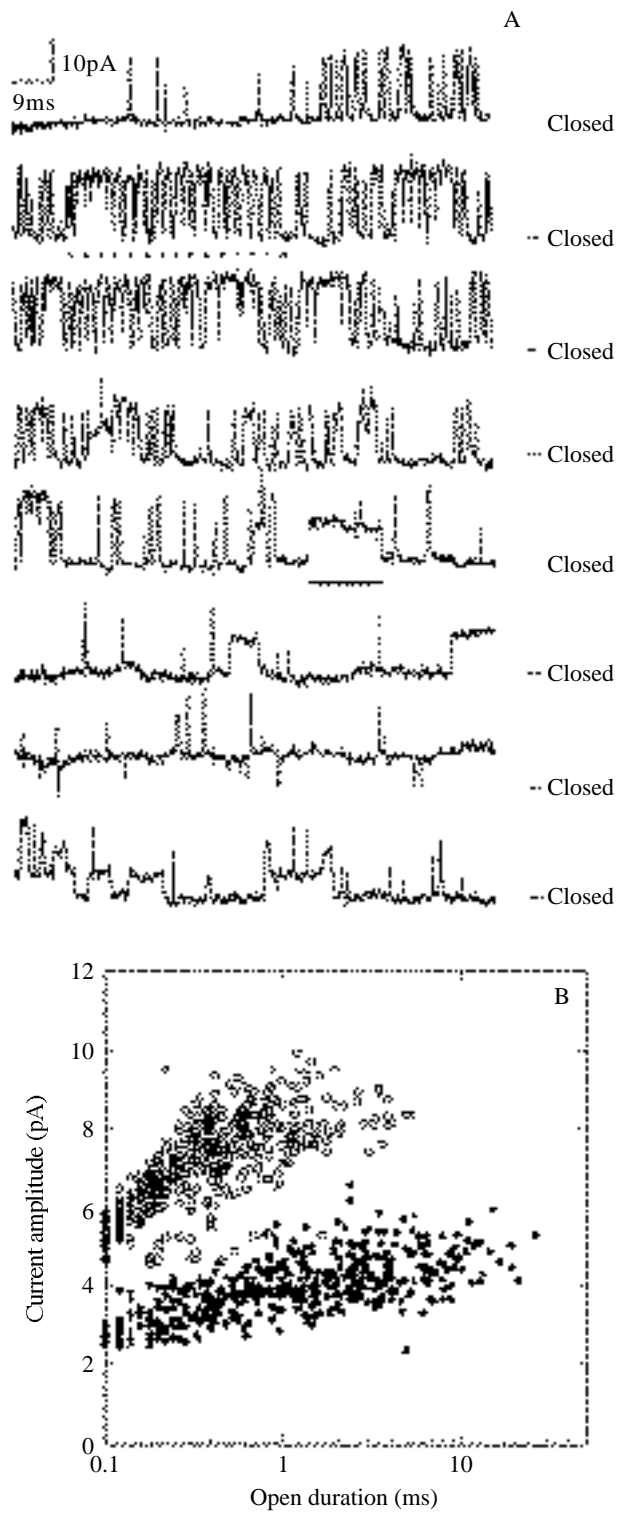


Fig. 5



classes of channels are active simultaneously in the bleb patches. In the recording illustrated, both large and small single-channel currents are prominent, with occasional multiple openings of both channel types.

The histogram in Fig. 4B illustrates the amplitude distribution of data points digitized from a 7.5s recording from the patch shown in Fig. 4A ( $-V_{\text{pipette}} +60\text{mV}$ ). Peak 1 (centered at 0pA) represents data recorded from the patch when all the channels were apparently closed (no transitions below this average baseline were recorded). From the area under the curve under peak 1 the percentage of time during which all channels are closed can be estimated as 31% of the total recording time. Curve-fitting of the histogram peaks to the right of peak 1 allows estimation of the size of several single-channel currents present in the recording. For example, peak 2 in Fig. 4B (centered at 6.32pA) represents openings of the smallest channel detected. The area under peak 2 reflects the high probability of finding this channel in the open state. At least two of the small channels are present in this patch, since double openings of the small channel are observed in the raw data of Fig. 4A. These double openings are represented by peak 3 (12.48pA) in Fig. 4B. The remaining peaks in the amplitude histogram account for a smaller proportion of the recording time and result from openings of the large channel as well as simultaneous openings of large and small channels.

#### *Characterization of single channel types*

To characterize the single-channel conductances of ion channels in bleb membranes a series of d.c. membrane potential shifts was applied to excised patches with channel activity. In 36 membrane patches the conductance of the bleb membrane ion channels was determined by measuring the slope of the relationship between the amplitude of the single-channel current and the applied voltage. In these experiments several different species of ion channels could be clearly distinguished on the basis of their single-channel conductance and kinetic properties.

A recording showing two channel types that are frequently observed together in a single patch is illustrated in Fig. 5A. One channel type has a larger conductance, is open for brief durations and shows intermittent bursts of intense activity (dotted line), while the second (solid line) has a smaller conductance and appears to open for significantly longer periods than the first. A quantitative analysis of over 520 openings of these two channel types at a  $-V_{\text{pipette}}$  of +100mV results in the plot of channel current amplitude *versus*

---

Fig. 5. (A) Two types of channels active in the same patch. The dotted line indicates examples of current deflections due to openings of the large channel. The solid line indicates an example of a single opening of a smaller channel.  $-V_{\text{pipette}} +100\text{mV}$ . (B) Amplitude scatterplot for independent analyses of two channel types in a single record from the experiment shown in A. Open circles are measurements of the larger channel (mean current amplitude  $7.01 \pm 0.05\text{pA}$ ; mean channel open time  $0.56 \pm 0.29\text{ms}$ ;  $N=522$  open events). Filled circles are measurements of the smaller channel (mean channel current  $3.82 \pm 0.03\text{pA}$ ; mean channel open time  $2.13 \pm 0.14\text{ms}$ ;  $N=538$  open events).  $-V_{\text{pipette}} +100\text{mV}$ . Open events were detected as current fluctuations that exceeded 50% of the difference between the baseline current level and the open channel amplitude level. Measurements of the amplitude of the current during each channel open event were determined in separate analyses for each of the two channel types.

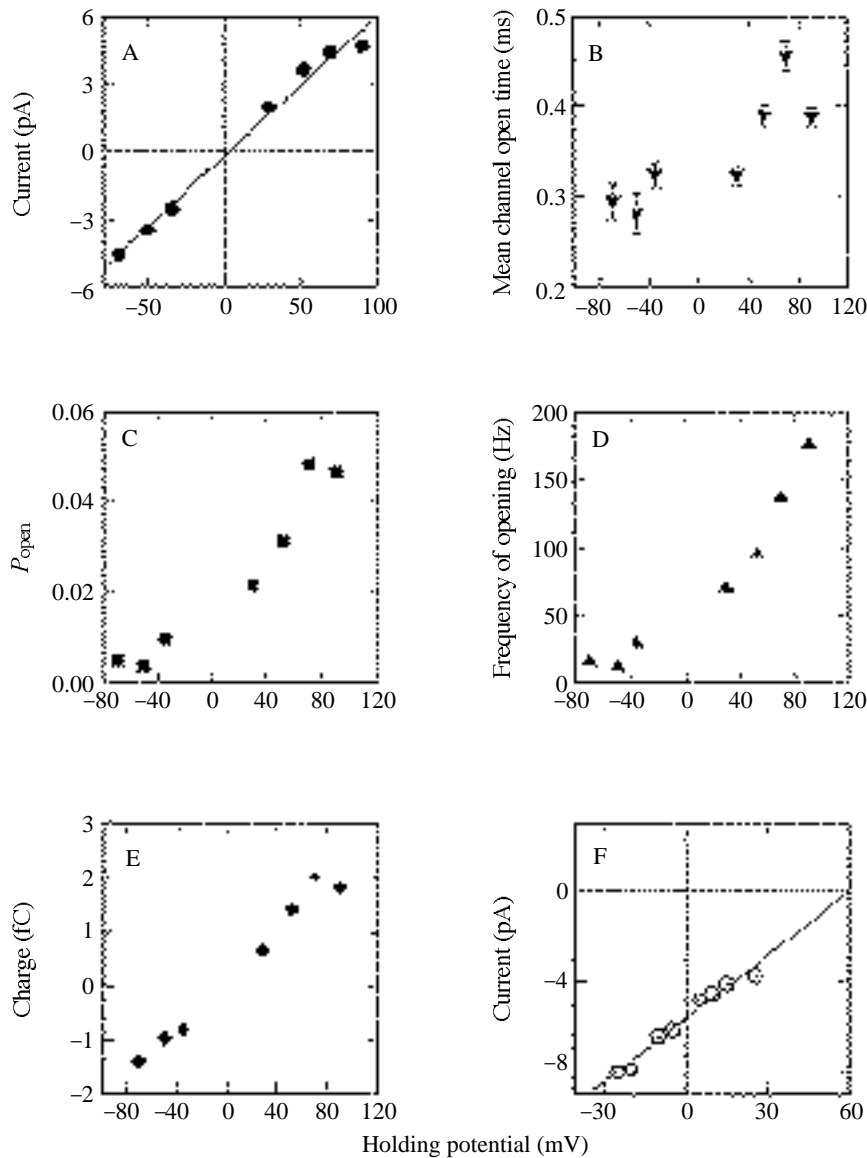


Fig. 6. (A)  $I-V$  relationship for the large channel shown in Fig. 5A. Each point represents the mean single-current amplitude ( $i$ ) measured from the distribution of over 400 open events at each voltage (error bars for each are not larger than the symbols). The single-channel conductance corresponds to the slope of the linear regression fitted to these points and is 62.8 pS. (B) Mean channel open time (MCOT) ( $\pm$  s.e.) as a function of voltage. Each point represents the mean duration of channel openings calculated for the same data as shown in A. (C) Probability of finding the channel in an open state ( $P_{open}$ ) as a function of voltage. (D) Frequency of channel opening as a function of voltage. (E) Predicted charge carried by the open channel (calculated as the product of MCOT and the single-channel current  $i$ ) (F)  $I-V$  relationship for the same channel when bath KCl is replaced by NaCl (462 mmol l<sup>-1</sup>). In all plots, holding potential is equal to  $-V_{pipette}$ .

mean channel open time (MCOT) shown in Fig. 5B. These data confirm that the open lifetimes of the larger of the two conductances (MCOT=0.56±0.29ms; open circles) is significantly shorter than that of the smaller (MCOT=2.13±0.14ms; filled circles) channel.

To examine the properties of these channels, the activity of each was analyzed independently. The  $I$ - $V$  relationship for the larger conductance channel is shown in Fig. 6A. The slope of the regression line indicates that the single-channel conductance for this channel is 62.8pS and that the  $I$ - $V$  relationship for this channel is linear in the range  $-75$ mV to  $+60$ mV and reverses at 0mV in symmetrical recording solutions. The single-channel conductance may show weak rectification at voltages greater than  $+60$ mV; however, data from other experiments on this channel are limited in this voltage range. In seven experiments under identical experimental conditions the mean single-channel conductance was  $68.1 \pm 7.7$ pS (mean  $\pm$  s.d.). The mean channel open time (MCOT) for this channel is brief, approximately 0.3–0.4ms (at  $-75$ mV) and shows a weak voltage-dependence, increasing by approximately 25% as  $-V_{\text{pipette}}$  is increased to  $+80$ mV (Fig. 6B). The probability of finding a channel of this conductance in an open state over the same voltage range is highly voltage-dependent: the open probability ( $P_o$ ) at  $+80$ mV is approximately 10-fold higher than  $P_o$  measured at values of  $-V_{\text{pipette}}$  of  $-75$ mV to  $-50$ mV (Fig. 6C). The increase in  $P_o$  can be accounted for by a nearly 10-fold increase in the frequency of channel openings (Fig. 6D). In Fig. 6E, the net positive charge carried when this channel is open is illustrated as the product of the mean channel open time and the single-channel current at various holding potentials. The profile of this channel is nearly linear over a range of membrane potentials from  $-50$ mV to  $+100$ mV.

To determine whether this channel displays ion selectivity, the  $462\text{mmol l}^{-1}$  KCl solution bathing the intracellular face of the patch was replaced with  $462\text{mmol l}^{-1}$  NaCl. In the presence of intracellular sodium the  $I$ - $V$  curve for this channel shifted to the right by  $+60$ mV (Fig. 6F). This observation suggests that the channel conducts cations and is highly selective for potassium compared with sodium. The mean permeability ratio  $P_{\text{K}}/P_{\text{Na}}$  was calculated from the reversal potential measured in four experiments and averaged 12:1, with a range of 16.7:1–10.1:1.

The  $I$ - $V$  relationship for the second channel is shown in Fig. 7A. The single-channel conductance is approximately 35.0pS, and the  $I$ - $V$  relationship is linear, reversing at 0mV under conditions where the bath and the pipette interior contain identical solutions. In 10 experiments under identical experimental conditions the mean single-channel conductance was  $40.5 \pm 5.4$ pS (mean  $\pm$  s.d.). The mean channel open time does not seem to be voltage-dependent and is approximately 2ms (Fig. 7B), more than four times larger than that of the 68pS channel described above. As with the larger channel, the probability of channel opening for the smaller channel increases at more depolarized potentials and correlates with an increase in the frequency of channel openings at depolarized voltages (Fig. 7C,D). The net positive charge carried through this channel is shown in Fig. 7E and is a linear function of the pipette potential. When the intracellular face of the patch is superfused with  $462\text{mmol l}^{-1}$  NaCl replacing KCl, the  $I$ - $V$  curve shifts to the right (Fig. 7F), suggesting that this channel is also a cation channel selective for potassium. In three experiments, the extrapolation of the reversal potential gave an average value of

+40mV in the presence of internal sodium, corresponding to an average value for  $P_K/P_{Na}$  of 4.9:1, with a range of 3.9:1–6.5:1.

In Fig. 8 the frequency of channel opening for each channel type is displayed as a function of time and pipette potential (both channels were active simultaneously in the same patch). The 40pS channel is active at all holding potentials, but opens more frequently at strongly depolarizing voltages (Fig. 8E). The 68pS channel displays little activity at negative holding potentials, with relatively long periods during which there are

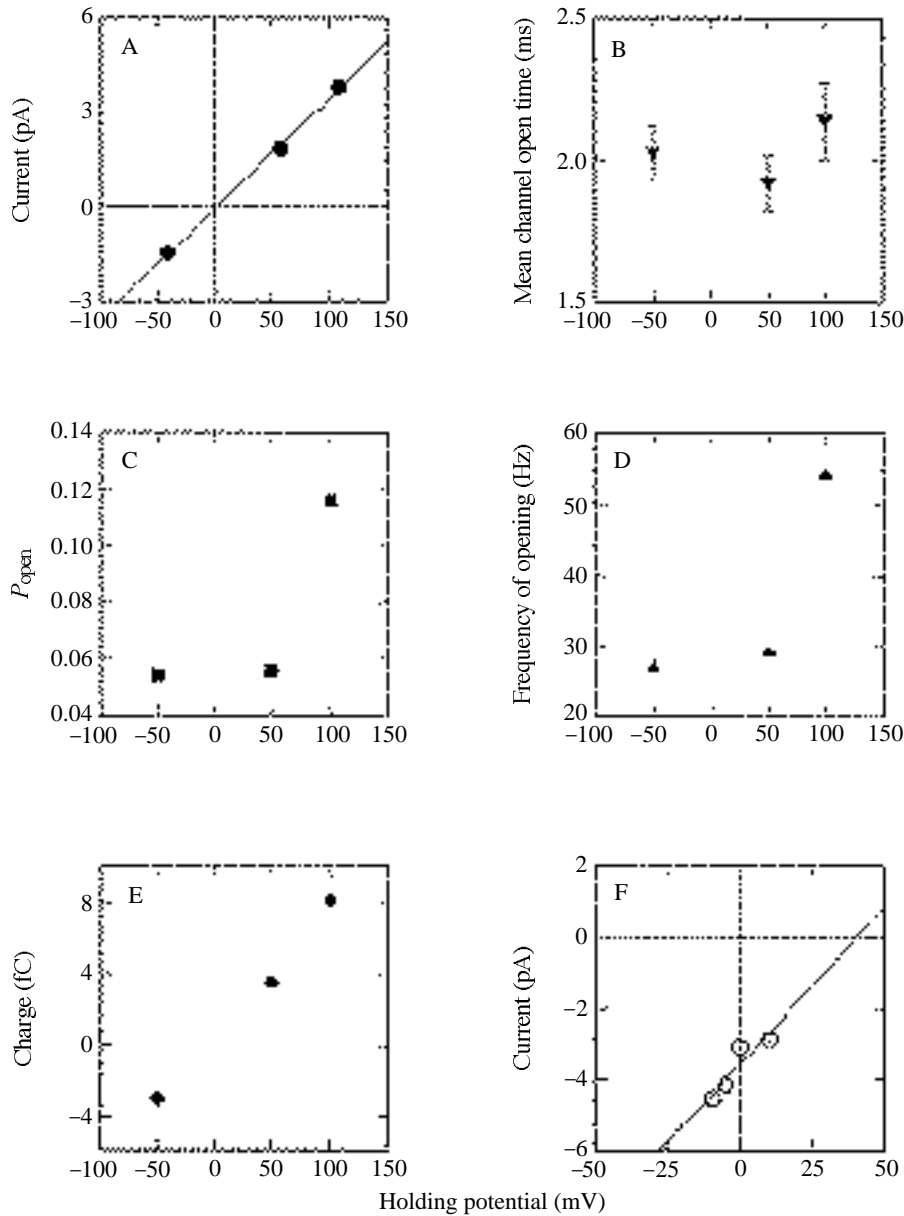


Fig. 7

no openings (Fig. 8B). This channel becomes increasingly active at depolarizing voltages, with periods of intense bursting at a  $-V_{\text{pipette}}$  of +100mV (Fig. 8F). The kinetic behavior of both types of channels suggests that the macroscopic current flow at steady state would demonstrate outward rectification, because of the increase in the probability of channel opening at depolarizing voltages (see also Figs 6C and 7C) and the lack of channel inactivation over long (10s) periods of maintained depolarization.

#### *The variety of channels in lobster skeletal muscle*

A summary histogram representing  $I-V$  analyses of 36 excised membrane patches recorded in symmetrical KCl solutions is shown in Fig. 9. The sizes of single-channel conductances observed in the blebs extend over an approximately tenfold range (32–380pS). Certain size classes of channels were observed repeatedly, with two size classes (32–45pS and 60–80pS) being recorded with the highest frequency. Larger channel conductances of 300–400pS were recorded less often. Patches displaying activity of these large channels often also showed channels of smaller conductances.

### Discussion

Many types of ion channels co-exist in the sarcolemma of lobster exoskeletal muscle fibers, even under the narrowly defined experimental conditions imposed in these experiments. A large range of single-channel conductances and distinct gating properties were observed from channels recorded under bi-ionic conditions where potassium was the only permeant cation. All the channels observed displayed nonrectifying single-channel  $I-V$  relationships in symmetrical recording solutions and were active in patches held for prolonged periods at d.c. holding potentials. All were active in the absence of exogenously added calcium, ATP or other intracellular messengers or metabolites.

The variety of single potassium channel types observed in this study of sarcolemmal blebs raises the issue of whether a similar diversity of channel types exists in intact muscle membrane. Preliminary experiments on intact muscle fibers indicate that several kinetically distinct channels with a range of single-channel conductances are active in recordings of excised inside-out patches of sarcolemmal membrane. The properties of the

---

Fig. 7. (A)  $I-V$  relationship for the small channel from the recording in Fig. 5A. Each point represents the mean single-channel current amplitude ( $i$ ) from over 367 open events measured at each voltage (error bars are not larger than the symbols). The single-channel conductance corresponds to the slope of the linear regression fitted to these points and is 35.0pS. (B) Mean channel open time (MCOT) ( $\pm$  S.E.) as a function of voltage. Each point represents the mean duration of channel openings calculated for the current measurements shown in A. (C) Probability of finding the channel in an open state ( $P_o$ ) as a function of voltage. Data are corrected for the fact that two channels of this type were active in the patch (the probability of a single channel being open is half of the total probability that any channel is open). (D) Frequency of channel opening as a function of voltage; data are corrected for the presence of two active channels. (E) Predicted charge carried by the open channel (calculated as the product of MCOT and the single-channel current  $i$ ). (F)  $I-V$  relationship for the same channel when bath KCl is replaced by NaCl (462mmol l<sup>-1</sup>). In all plots, holding potential is equal to  $-V_{\text{pipette}}$ .

channels in the intact preparations have not been studied in detail; however, it seems unlikely that the variety of channels described in this study of membrane blebs arises simply from the loss of cytoskeletal and intracellular regulatory influences.

Lobster skeletal muscle membranes are not unique in showing a broad diversity of

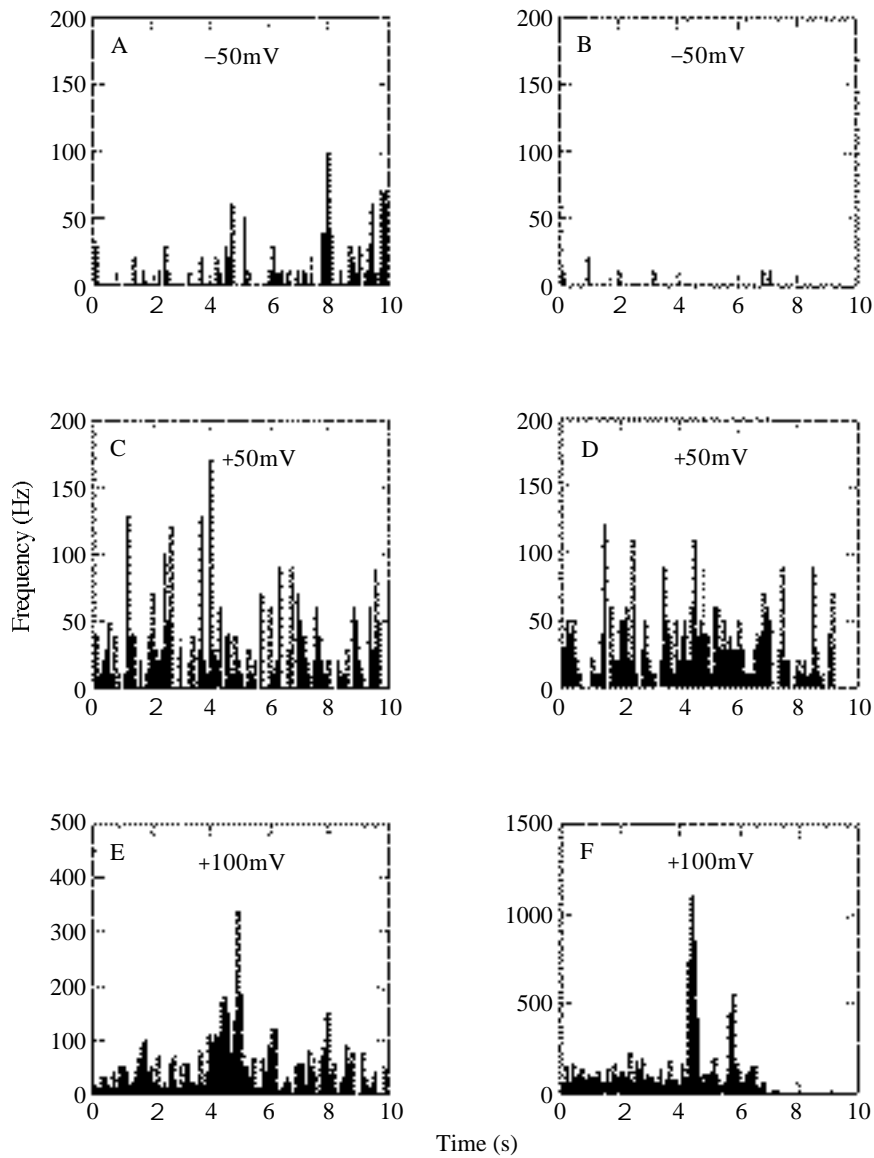


Fig. 8. Frequency plots of channel activity from the recording in Fig. 5. (A,C,E) Spontaneous activity of the 40pS channel (two channels of this type are active in this patch). (B,D,F) Spontaneous activity of the 68pS channel (one channel of this type is active in the patch). Data are represented as the frequency of channel opening observed in each 100ms bin over a recording period of 10s at each holding potential. (Note that the y-axis is rescaled for each channel at a  $-V_{\text{pipette}}$  of +100mV.)

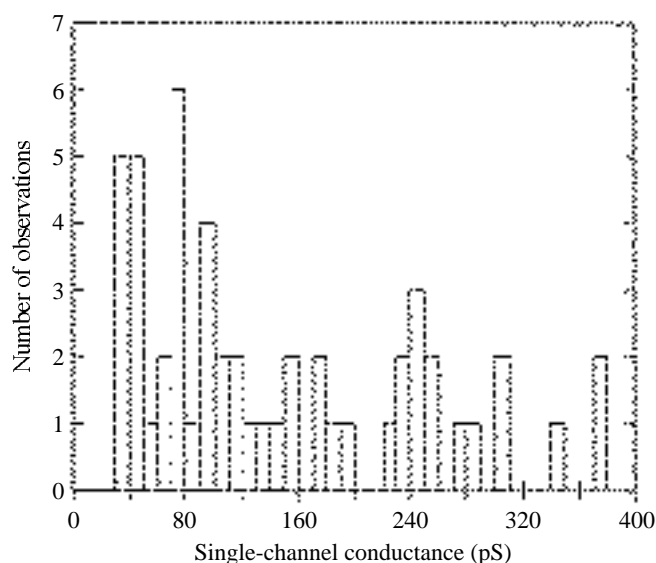


Fig. 9. Histogram of single-channel conductances recorded under symmetrical bi-ionic conditions ( $462\text{mmol l}^{-1}$  KCl) from lobster sarcolemmal bleb membrane ( $N=52$  conductances in 36 patches). Binwidth is 20pS.

potassium-selective ion channel types. A variety of channel types has also been reported in other studies in which invertebrate muscle potassium channels have been characterized at the single-channel level. For example, in cultured embryonic locust myofibers, five potassium channel types have been described; three of these are inward rectifiers and one is calcium-dependent (Miller and Usherwood, 1990). In *Drosophila melanogaster* muscle, a number of potassium channels are expressed over the course of development, including the depolarization-activated transient  $I_A$  current (Salkoff, 1983; Solc *et al.* 1987; Zagotta *et al.* 1988). Other *Drosophila* muscle potassium channels described at the single-channel level include stretch-activated, voltage-dependent and calcium-dependent channel types (Wu and Ganetzky, 1988; Zagotta *et al.* 1988). In crayfish stomatogastric muscle, a calcium-independent depolarization-activated potassium channel has been reported (Franke *et al.* 1986).

The two channels described in detail in this study show a high frequency of opening at depolarizing holding potentials, suggesting that they carry outwardly rectifying macroscopic currents in the intact muscle fiber. The  $I-V$  relationships for both single-channel conductances are ohmic. Therefore, the rectification of the macroscopic currents appears to arise from the voltage-dependence of channel open-state probability and not from non-linearities in the  $I-V$  relationships of the single-channel conductances. Both channels demonstrate non-inactivating activity at maintained holding potentials, consistent with the possibility that these channels may be delayed rectifiers. However, further experiments will be required to confirm this possibility. The voltage-sensitivity of the predicted macroscopic current flow through both channels suggests that the outward current is substantial at transmembrane voltages greater than 0mV. Under normal physiological conditions, the membrane potential of lobster muscle fibers does not reach

positive potentials, since these membranes carry no sodium spikes and contractions are graded and proportional to depolarization. However, under the influence of amines and the peptide proctolin, overshooting calcium action potentials appear in lobster exoskeletal muscle fibers (Kravitz *et al.* 1980). Under such conditions, the two channels described here would be activated and could serve an important role in repolarizing the muscle membrane potential.

Further studies will be required to determine how the channels described in this study relate to macroscopic potassium currents previously reported in lobster exoskeletal muscle. Earlier preliminary studies indicated that these fibers exhibit a tetraethylammonium (TEA<sup>+</sup>)-sensitive potassium current, a calcium-dependent potassium current and a potassium current insensitive to TEA<sup>+</sup> (Kravitz *et al.* 1980). It is not known whether the channel types described here are sensitive to TEA<sup>+</sup> or whether these channels might be sensitive to calcium (no calcium chelators were used in this study). Potassium channels are important targets for modulation in other systems, where they play significant roles in determining the resting membrane potential and the rate of repolarization after excitatory input (Siegelbaum *et al.* 1982; Belardetti *et al.* 1987; Wakatsuki *et al.* 1992; Escande and Cavero, 1992). In lobster muscle, neurohormonal regulation of potassium-selective channels could be critical in controlling the muscle membrane potential, thereby directly influencing muscle fiber excitability and contractility.

The authors gratefully acknowledge the technical assistance of Ms Nicole Cherbuliez. This investigation was supported by Project 1 of a Program Project Grant (NS25915; E.A.K., Principal Investigator) and by grants from the US–Israel Binational Science Foundation and Muscular Dystrophy Association. M.K.W. was the recipient of an NRSA (5F32NS08605) and a Grass Foundation Fellowship (Marine Biological Laboratory, Woods Hole).

### References

- ATWOOD, H. L., DIXON, D. AND WOJTCWICZ, J. M. (1989). Rapid introduction of long lasting synaptic changes at crustacean neuromuscular junctions. *J. Neurobiol.* **20**, 373–385.
- BATELLE, B. A. AND KRAVITZ, E. A. (1978). Targets of octopamine action in the lobster: cyclic nucleotide changes and physiological effects in hemolymph, heart and exoskeletal muscle. *J. Pharmac. exp. Ther.* **205**, 438–448.
- BELARDETTI, F., KANDEL, E. R. AND SIEGELBAUM, S. A. (1987). Neuronal inhibition by the peptide FMRFamide involves opening of 'S' K<sup>+</sup> channels. *Nature* **325**, 153–156.
- BISHOP, C. A., KROUSE, M. E. AND WINE, J. J. (1991). Peptide cotransmitter potentiates calcium channel activity in crayfish skeletal muscle. *J. Neurosci.* **11**, 269–276.
- BREEN, C. A. AND ATWOOD, H. L. (1983). Octopamine – a neurotransmitter with presynaptic activity dependent effects at crayfish neuromuscular junctions. *Nature* **303**, 716–718.
- BURTON, F., DORSTELMANN, U. AND HUTTER, O. F. (1988). Single channel activity in sarcolemmal vesicles from human and other mammalian muscle. *Muscle and Nerve* **11**, 1029–1038.
- DIXON, D. AND ATWOOD, H. L. (1989b). Conjoint action of phosphatidylinositol and adenylate cyclase systems in serotonin-induced facilitation at the crayfish neuromuscular junction. *J. Neurophysiol.* **62**, 1251–1259.
- DIXON, D. AND ATWOOD, H. L. (1989a). Phosphatidylinositol system's role in serotonin-induced facilitation at the crayfish neuromuscular junction. *J. Neurophysiol.* **62**, 239–246.



- DUDEL, J. (1965). Facilitatory effects of 5-hydroxytryptamine on the crayfish neuromuscular junction. *Naunyn-Schmiedeberg's Arch. Pharmacol.* **249**, 515–528.
- ESCANDE, D. AND CAVERO, I. (1992). K<sup>+</sup> channel openers and 'natural' cardioprotection. *Trends Pharmacol. Sci.* **13**, 269–272.
- EUSEBI, F., FARINI, F., GRASSI, L., MONACO, L. AND RUZZIER, F. (1988). Effects of calcitonin gene-related peptide on synaptic acetylcholine receptor-channels in rat muscle fibres. *Proc. R. Soc. Lond. B* **234**, 333–342.
- EVANS, P. D., KRAVITZ, E. A., TALAMO, B. R. AND WALLACE, B. G. (1976). The association of octopamine with specific neurons along lobster nerve trunks. *J. Physiol., Lond.* **262**, 51–70.
- EVANS, P. D., TALAMO, R. B. AND KRAVITZ, E. A. (1975). Octopamine neurons: morphology, release of octopamine and possible physiological role. *Brain Res.* **90**, 340–347.
- FISCHER, L. AND FLOREY, E. (1983). Modulation of synaptic transmission and excitation-contraction coupling in the opener muscle of the crayfish, *Astacus leptodactylus*, by 5-hydroxytryptamine and octopamine. *J. exp. Biol.* **102**, 187–198.
- FRANKE CH., HATT, H. AND DUDEL, J. (1986). The excitatory glutamate-activated channel recorded in cell-attached and excised patches from the membrane of tail, leg and stomach muscles of crayfish. *J. comp. Physiol. A* **159**, 579–589.
- FRIEL, D. D. AND BEAN, B. P. (1988). Two ATP-activated conductances in bullfrog atrial cells. *J. gen. Physiol.* **91**, 1–27.
- GOY, M. F. AND KRAVITZ, E. A. (1989). Cyclic AMP only partially mediates the actions of serotonin at lobster neuromuscular junctions. *J. Neurosci.* **9**, 369–379.
- GRUNDFEST, H. AND REUBEN, J. P. (1961). Neuromuscular synaptic activity in lobster. In *Nervous Inhibition* (ed. E. Florey), pp. 92–104. New York: Pergamon Press.
- HAMILL, O. P., MARTY, A., NEHER, E., SAKMANN, B. AND SIGWORTH, F. J. (1981). Improved patch-clamp techniques for high-resolution current recording from cells and cell-free membrane patches. *Pflügers Arch.* **391**, 85–100.
- KOBIERSKI, L. A., BELTZ, B. S., TRIMMER, B. A. AND KRAVITZ, E. A. (1987). The FMRFamide-like peptides of *Homarus americanus*: distribution, immunocytochemical mapping and ultrastructural localization in terminal varicosities. *J. comp. Neurol.* **266**, 1–15.
- KRAVITZ, E. A., BELTZ, B. S., GLUSMAN, S., GOY, M. F., HARRIS-WARRICK, R. M., JOHNSTON, M., LIVINGSTONE, M. S., SCHWARZ, T. AND SIWICKI, K. K. (1985). The well-modulated lobster: the roles of serotonin, octopamine and proctolin in the lobster nervous system. In *Model Neural Networks and Behavior* (ed. A. Selverston), pp. 339–360. New York: Plenum Press.
- KRAVITZ, E. A., GLUSMAN, S., HARRIS-WARRICK, R. M., LIVINGSTONE, M. S., SCHWARZ, T. AND GOY, M. F. (1980). Amines and a peptide as neurohormones in lobsters: actions on neuromuscular preparations and preliminary behavioural studies. *J. exp. Biol.* **89**, 159–175.
- LIVINGSTONE, M. S., HARRIS-WARRICK, R. M. AND KRAVITZ, E. A. (1980). Serotonin and octopamine produce opposite postures in lobsters. *Science* **208**, 76–79.
- LIVINGSTONE, M. S., SCHAEFFER, S. F. AND KRAVITZ, E. A. (1981). Biochemistry and ultrastructure of serotonergic nerve endings in the lobster: serotonin and octopamine are contained in different nerve endings. *J. Neurobiol.* **12**, 27–54.
- MERCIER, A. J., SCHIEBE, M. AND ATWOOD, H. L. (1990). Pericardial peptides enhance synaptic transmission and tension in phasic extensor muscles of crayfish. *Neurosci. Lett.* **111**, 92–98.
- MILLER, B. A. AND USHERWOOD, P. N. R. (1990). Characteristics of five types of K<sup>+</sup> channels in cultured locust muscle. *J. exp. Biol.* **154**, 45–65.
- SALKOFF, L. B. (1983). Genetic and voltage-clamp analysis of a *Drosophila* potassium channel. *Cold Spring Harbor Symp. quant. Biol.* **48**, 221–231.
- SCHWARZ, T. L., HARRIS-WARRICK, R. M., GLUSMAN, S. AND KRAVITZ, E. A. (1980). A peptide action in a lobster neuromuscular preparation. *J. Neurobiol.* **11**, 623–628.
- SCHWARZ, T. L., LEE, G. M., SIWICKI, K. K., STANDAERT, D. G. AND KRAVITZ, E. A. (1984). Proctolin in the lobster: the distribution, release and chemical characterization of a likely neurohormone. *J. Neurosci.* **4**, 1300–1311.
- SIEGELBAUM, S. A., CAMARDO, J. S. AND KANDEL, E. R. (1982). Serotonin and cyclic AMP close single K<sup>+</sup> channels in *Aplysia* sensory neurons. *Nature* **299**, 413–417.
- SOLC, C. K., ZAGOTTA, W. N. AND ALDRICH, R. W. (1987). Single-channel and genetic analysis reveal two distinct A-type potassium channels in *Drosophila*. *Science* **236**, 1094–1098.

- SULLIVAN, R. E. (1978). Stimulus-coupled serotonin release from identified neurosecretory fibers in the spiny lobster, *Panulirus interruptus*. *Life Sci.* **22**, 1429–1437.
- SULLIVAN, R. E., FRIEND, B. J. AND BARKER, D. L. (1977). Structure and function of spiny lobster ligamental nerve plexuses: Evidence for synthesis, storage and secretion of biogenic amines. *J. Neurobiol.* **8**, 581–605.
- TRIMMER, B. A., KOBIERSKI, L. A. AND KRAVITZ, E. A. (1987). Purification and characterization of FMRFamide-like immunoreactive substances from the lobster nervous system: Isolation and sequence analysis of two closely related peptides. *J. comp. Neurol.* **266**, 16–26.
- WAKATSUKI, T., NAKAYA, Y. AND INOUE, I. (1992). Vasopressin modulates K<sup>+</sup>-channel activities of cultured smooth muscle cells from porcine coronary artery. *Am. J. Physiol.* **263**, H491–H496.
- WU, C.-F. AND GANETZKY, B. (1988). Genetic and pharmacological analyses of potassium channels in *Drosophila* muscle. In *Neurotox '88, Molecular Basis of Drug and Pesticide Action* (ed. G. Lunt). Internal Congress Series **832**, pp. 311–325.
- ZAGOTTA, W. N., BRAINARD, M. S. AND ALDRICH, R. W. (1988). Single-channel analysis of four distinct classes of potassium channels in *Drosophila* muscle. *J. Neurosci.* **8**, 4765–4779.